Research Article

Journal of Environmental Nanotechnology

Photocatalytic Degradation of Azo Dyes by Pure and Aluminium-doped Cadmium Oxide Nanocrystalline Thin Films

V. Radhika[1*], V. Annamalai[2]

[1]P.K.R Arts College for Women, Gobichettipalayam, TN, India
[2]P.S.G College of Arts and Science, Coimbatore, TN, India
Received: 25.11.2020 Accepted: 25.12.2020 Published: 30-12-2020
*radhikaviswanath@gmail.com

ABSTRACT

Pure and Al-doped Cadmium oxide nanocrystalline thin films were synthesized by using the chemical bath deposition method and annealed at 500 ºC. The films were characterized to study their structural, optical and compositional properties. The films were used to degrade the azo dyes, methylene blue (MB) and methyl orange (MO) using photocatalytic activity (PCA). It was found that the films were capable of degrading MB up to 19% and were able to decolorize MO up to 30%.

Keywords: Al-doped CdO; Azo dyes; Cadmium oxide; Photo-catalytic activity.

1. INTRODUCTION

Organic chemicals found as pollutants in wastewater effluents from industrialized sources must be destroyed before discharging to the environment. Such pollutants may also be found in ground and surface waters which also need treatment to achieve acceptable drinking water quality. Among various methods, photo catalysis has gained prominent notice in the field of pollutant degradation.

One of the major advantages of the photo catalytic process is that there is no additional requirement for secondary disposal. Another benefit lies in the fact that when compared to other advanced oxidation technologies, especially those using oxidants such as hydrogen peroxide and ozone, expensive oxidizing chemicals are not required as ambient oxygen is the oxidant (Rajachandrasekar, *et al.* 2016). Photocatalysts are also self-regenerated and can be reused or recycled.

Photo-catalysis is the acceleration of a photoreaction in the presence of a catalyst. In catalyzed photolysis, light is absorbed by an adsorbed substrate. In photo-generated catalysis, photo catalytic activity (PCA) depends on the capability of the catalyst to generate electron–hole pairs, which creates free radicals (e.g., hydroxyl radicals: -OH) that are capable of experiencing secondary reactions. A reaction between the excited electrons with an oxidant to convert a reduced product to an oxidized product takes place. Due to the generation of positive holes and electrons, oxidation-reduction reactions take place on the surface of semiconductors. In the oxidative reaction, the positive holes respond with the moisture present on the surface and generate a hydroxyl radical. Oxidative reactions due to photocatalytic effect are as follows:

$$UV + MO \rightarrow MO\ (h + e^{-})$$
(Here, MO represents Metal Oxide)
$$h^{+} + H_2O \rightarrow H^{+} + \text{-OH}$$
$$2\ h^{+} + 2H_2O \rightarrow 2H^{+} + H_2O_2$$
$$H_2O_2 \rightarrow 2(\text{-OH})$$

The reductive reaction due to photocatalytic effect:

$$e^{-} + O_2 \rightarrow \text{-}O_2^{-}$$
$$\text{-}O_2^{-} + (HO\text{-})_2 + H^{+} \rightarrow H_2O_2 + O_2$$
$$HOOH \rightarrow HO^{-} + \text{-OH}$$

Requirements for an efficient photo catalytic material include: (i) an ability to generate electron-hole pairs and prevent re-combination long enough for the electrons and holes to reach the surface of the thin film, (ii) activation by sunlight (iii) inexpensive and easy means to produce (iv) chemically inert and (v) physically adherent and strong.

Henamsylvia Devi and Thsiyam David Singh prepared Copper nanoparticles using *Centellaasiatica L.* leaf extract at room temperature for the photocatalytic degradation of methyl orange. These nanoparticles reduced methyl orange to its leuco form in aqueous medium in the absence of reducing agents. This catalytic effect of copper oxide nanoparticles contributed to its small size. Copper oxide nanoparticles as prepared had

good catalytic properties. Beydoun *et al.* 1998 gave an overview of the development and implications of nanotechnology in photo catalysis and the use of nanocrystalline thin films in electrochemically-assisted photocatalytic processes.

2. EXPERIMENTAL METHODS

2.1 Synthesis of pure and Al-doped CdO thin films

In the present work, Cadmium Oxide (CdO) thin films were prepared on glass substrates by Sol-gel chemical bath deposition technique. In a conical flask, 0.1 M of Cadmium chloride ($CdCl_2.2½H_2O$) was dissolved in 250 ml of deionized water. The solution was continuously stirred by a magnetic stirrer for 1 hour to get a clear homogeneous solution. Ammonium hydroxide ($NH_3.H_2O$) solution was added with this solution drop-wise till the pH value reached 12. The solution is taken in small beakers and the glass substrates were immersed to about 5 cm into beakers for 24 hours. The glass slides were dried in a hot air oven. These slides were annealed to 500 ºC. The undoped CdO thin film was prepared. The same procedure was followed to dope aluminum to CdO. Anhydrous aluminum chloride ($AlCl_3$) was added to the pure CdO precursor in the beaker (Hajjaji, *et al.* 2014). The results obtained for the lesser concentrations of 1% and 2% of Al-doping exhibit similar results for XRD analysis. Hence, 3 wt. % Al-doping was optimized. This solution is stirred using a magnetic stirrer for 2 hours. The glass substrates were dipped into the beaker for 24 hours.

$$CdCl_2 + 4NH_3 .H_2O \rightarrow [Cd(NH_3)_4]_2^+ + 4OH^- + 2Cl^- + 4H_2O$$
$$2Cd_2^+ + 3OH^- \rightarrow 2CdO + H_2O$$
$$Al(H_2O)_6 Cl_3 \rightarrow Al(OH)_3 + 3HCl + 3H_2O$$

Aluminum Oxide is formed from the Aluminum Hydroxide on strong heating (~400 ºC) via:

$$2\ Al(OH)_3 \rightarrow Al_2O_3 + 3H_2O$$

The glass substrates were dried using a hot air oven and annealed at 500 ºC.

Al was chosen as a dopant to organize and improve the properties of CdO thin films. Al^{3+} ion has three valence electrons and the ionic radius of Al^{3+} ion (0.68 Å) is slightly smaller than that of Cd^{2+} ion (0.95 Å). Thus Al^{3+} ion-doping in CdO will enhance the electrical conductivity by increasing electron concentration (Saleh *et al.* 2012). Since Al^{3+} has a lesser ionic radius than that of Cd^{2+}, there would be a significant difference in its electrical property (Tadjarodi *et al.* 2014). This is attainable by a shift in the optical band gap along with the enhancement in the transparency of CdO films (Beydoun *et al.* 1998).

2.2 Photo-catalytic Activity Test

The photocatalytic activity of CdO nanoparticles can be studied using methylene blue [$C_{16}H_{18}ClN_3S$] and methyl orange [$C_{14}H_{14}N_3NaO_3S$], the widely used azo dyes. The CdO thin films synthesized were dipped in methylene blue and methyl orange solutions. The methylene blue was examined by using a V-Visible Spectrophotometer. The maximum absorption was found to be at a wavelength of 675 nm. The maximum absorbance of MB is around 66-665 nm (Lajnef *et al.* 2007; Cheng *et al.* 2013). Methyl orange solution was treated with UV-Visible light, which gave a maximum absorption at a wavelength of 465 nm. The maximum absorbance of methyl orange is approximately 462 nm in the visible region. The concentration of both dyes were prepared to be 10 ppm. Irradiation of the solutions was carried out under UV-Vis. light (6 lamps with a power of 20 W, Philips).

The experiment was executed as follows: The maximum absorbance of both methylene blue solution and methyl orange solution were measured and then the wavelength. Absorbance was noted for the degradation of the dye before and after the addition of metal oxide. This absorbance is noted to be A_o. After UV irradiation, the absorbance was again measured at 't' intervals of time. For every hour, the absorbance value is noted. The total irradiation time is 5 hours. The extent of the photocatalytic activity of CdO in methylene blue and methyl orange can be determined by measuring the absorbance of the solutions. The degradation of the dyes can be evaluated by using the formula:

$$\text{Degradation (\%)} = [(A_0 - A_t)/A_0] \times 100$$

where, A_0 represents the initial absorbance and A_t represents the absorbance after 't' min. reaction of the dyes at the characteristic absorption wavelength of 675 nm.

According to the principles of CdO photo catalyst, an energy gap is created on the surface of Cadmium oxide when photon light radiation is given with either greater than or equal to the bandgap energy, and an electron may be advanced from the valence band to the conduction band (e^- c_b) leaving behind an electronic vacancy or "hole" in the valence band (h^+ v_b). If charge separation is sustained, the electron and hole may transfer to the catalyst surface, where they take part in redox reactions with the sorbed species.

3. RESULTS AND DISCUSSION

3.1. X-Ray Diffraction Analysis

The structural properties of CdO nanoparticles were investigated using an X-ray diffraction analysis.

The existence of multiple diffraction peaks of (011), (111), (200), (220), (311) and (222) planes specifies the polycrystalline nature of the CdO with cubic structure (Comparelli *et al.* 2005). The XRD pattern exposed diffraction peaks approximately at 33º, 38º, 55.5º and 68º of 2θ values, indicating the hkl values as (1 1 1), (2 0 0), (2 2 0) and (2 2 2), which correspond to polycrystalline having the characteristic peaks of face-centered cubic structure of CdO (JCPDS Card No. 05-0640, 73-2245 and 78-065) (Hussein *et al.* 2013; Hamadanian *et al.* 2013; Harraz *et al.* 2014) as shown in Fig. 1 (a).

The sharp peak values are used to calculate the lattice parameter and grain size. Doping CdO films with Al causes a small reduction in the intensity of all peaks and especially of the (2 0 0) plane, as shown in Fig. 1 (b). The Al-doped CdO films have (1 1 1) plane as the preferred orientation and it is similar to the results reported by Hussein *et al.* 2013. The crystalline nature and the intensity of the peak of (1 1 1) in the diffraction pattern increase with an increase in Al-doping concentration, showing that the doping helps in the nucleation and growth of grains. The crystallite size (D) was calculated from the full width at half-maximum (FWHM) β of the major XRD peaks using Scherer-Bragg's relation (Jiang *et al.* 2013).

3.2 Morphological Analysis

SEM images of pure and Al-doped CdO thin films are shown in Fig. 2. A careful observation of pure CdO surface shows grains like mounts without well-defined boundaries. It can be seen that grains clump together and hence do not display homogeneous distribution for pure CdO samples. Average grain size could not be calculated due to clumping (Lee *et al.* 2014). The particle size is in the range of few nanometers and it exhibits needle-like structure for Al-doped CdO nanopowder. It is observed that the doping of Al stimulates an obvious change in grain size. Furthermore, the influence of incorporating Al on the surface morphology of the samples can be clearly seen (Nag *et al.* 2008; Borhade *et al.* 2012).

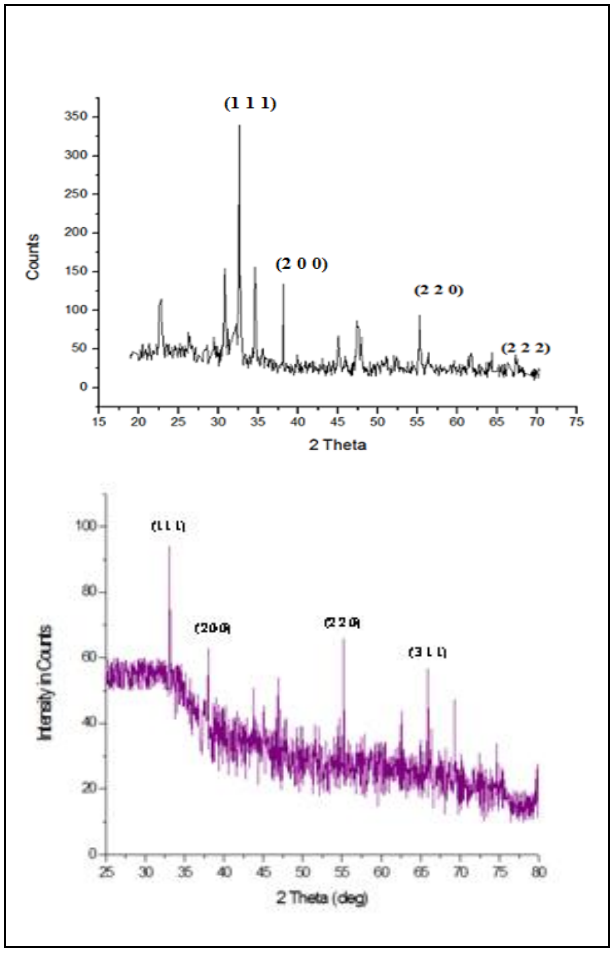

Fig. 1: XRD Spectrum of: (a) pure and (b) Al-doped CdO thin films.

Table 1. Structural values of CdO films

Film	2θ (deg)	FWHM (radians)	Lattice strain	Dislocation density ×10^{14} (δ) lines/m^2	Micro strain(ε) (10^4 lin^{-2}m^{-4})	Average crystallite size (D) in nm
Pure CdO	15.2526 18.3321 22.6727 26.3868 29.0478	0.3444 0.1476 0.1968 0.5904 0.1476	0.0225 0.0080 0.0087 0.0223 0.0051	17.1319 03.1414 05.5651 49.9450 03.1105	9.0365 8.7565 6.8558 4.2314 5.5734	38.76
Al:CdO 3wt%	5.7385 18.2243 31.8419 66.5304 84.4461	0.5063 0.5196 0.1299 0.9092 0.2598	0.0882 0.0285 0.0041 0.0133 0.0029	37.18024 38.91642 2.401467 110.1068 8.524695	20.67552 6.48847 5.160884 1.422715 4.87948	28.148

3.3 Photo-catalytic Degradation of Azo Dyes of Pure and Al-doped CdO Thin Films

Fig. 3 (a) shows the absorbance spectrum of methylene blue (MB) dye degradation using pure Cadmium Oxide thin films under the irradiation of UV light. From the figure it is clear that the absorbance of MB is more or less equal to 670 nm. When the CdO thin films are dipped for about 4 cm in the freshly prepared MB solution and kept under irradiation of UV light, it is monitored that the absorbance is considerably decreased. The irradiation time is varied from 1 hour to 5 hours. The absorbance value starts decreasing from the first hour of irradiation; at the fifth hour, the absorbance is found to be reduced significantly. At the first hour of light irradiation, decolorizing efficiency for MB dye solution was achieved to about 11%. This value nearly reached 18% after 5 hours of illumination. This result proves that the synthesized photo-catalyst performs remarkably in removing the mentioned azo dyes under visible light illumination in a short time.

In heterogeneous photo catalysis of azoic dyes, the electron-hole pairs will be primarily created by the irradiation of a semiconductor with a photon of energy equal to or better than its bandgap width (Cheng *et al.* 2013). The electrons and holes may drift to the semiconductors on the catalyst surface, where they participate in redox reactions with the adsorbed azoic dyes (Ullah *et al.* 2014). The oxidizing radical could hit the azo dye molecule and disintegrate it into CO_2 and H_2O molecules which are non-hazardous (Soltani *et al.* 2013; Ullah *et al.* 2014). It has been recommended that the formation of free radicals acts as a major oxidizing type (Comparelli *et al.* 2005). In the absence of catalyst, decolorization of MB and MO was not observed even after 24 hours, signifying that there was no direct oxidation path. On the other hand, decolorization of MB and MO happened only when CdO was brought into the solution mixtures indicating the essentiality of the films for promoting the decolorization, which perhaps takes place through the free radicals pathway.

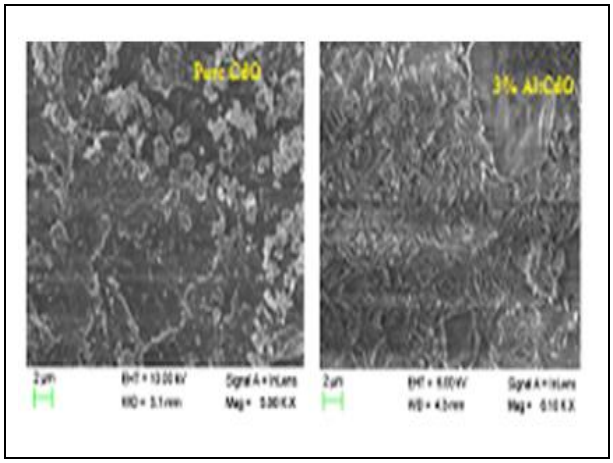

Fig. 2: SEM images of pure and Al-doped CdO thin films

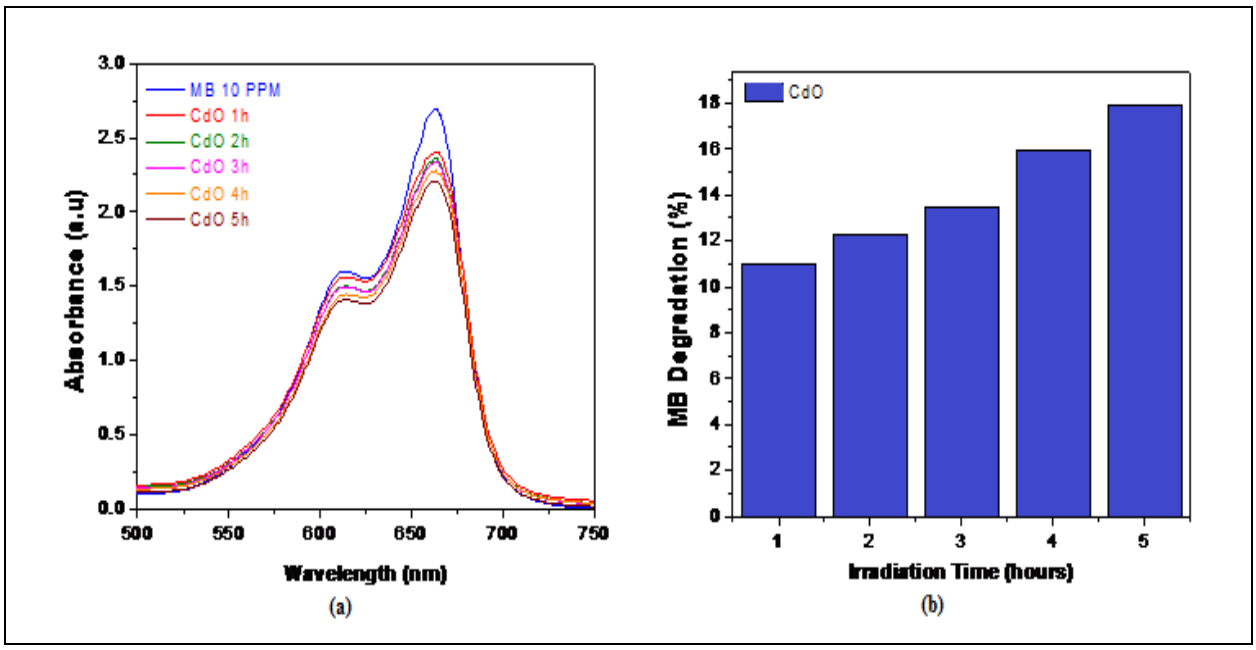

Fig. 3: Absorbance spectrum of MB dye degradation of: (a) pure CdO thin films (b) bar chart of MB degradation by pure CdO

The Fig. 4 (a) and (b) demonstrate the absorbance of MB by 3 wt. % Al-doped CdO thin films. To demonstrate the degradation process, the range was recorded at various time intervals. After an illumination time of 1 hour, the dye solution MB was destructed by 3 wt. % Al-doped CdO thin films by about 6%. The photo-catalytic process was prolonged for a few more hours, and the maximum degradation of the dye reached 18% after 5 hours. The MB reacts with the electrons generated on the CdO particles under UV irradiation.

Fig. 5 (a) explains the absorbance spectrum of Methyl Orange (MO) by pure CdO thin films. The absorbance of MO is at a wavelength of nearly 465 nm in visible light. When MO is treated with pure CdO thin films, there is only a slight variation in the absorbance value. The introduction of the thin films may assist the formation of OH^- radical through which the degradation of the dye proceeds. In order to exhibit the degradation process, the spectra were recorded at different time intervals.

In the absence of a photocatalyst, no degradation of azo dyes was observed under visible light irradiation (Tadjarodi *et al.* 2014). The obtained result also shows that when the CdO thin films were not introduced, there was no degradation of MB and MO under UV and visible irradiation.

The absorbance of MO by Al-doped CdO thin films is depicted by Fig. 6 (a and b). There is a vast decline in the absorbance of MO by 3 wt. % Al-doped CdO films with 5 hours of irradiation. At the beginning of UV irradiation, one can see that there is only 12.5% of photocatalytic degradation of MO. Later, as time progresses, 3 wt. % Al-doped CdO thin films illustrate a maximum of 30% of MO degradation, which is more than double the initial value.

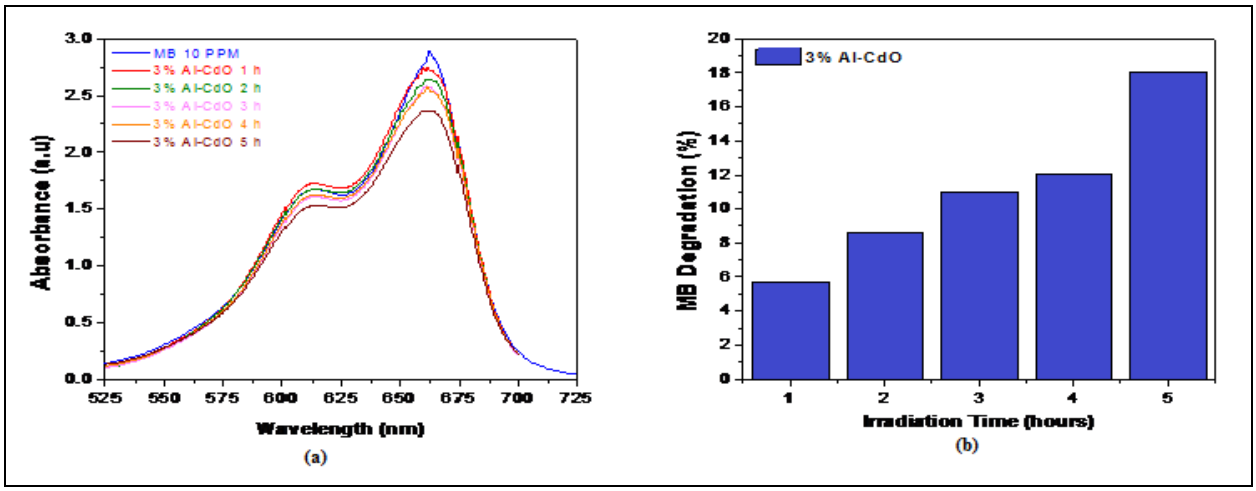

Fig. 4: (a) Absorbance of MB dye by 3 wt. % Al-doped CdO thin films and (b) the corresponding bar chart

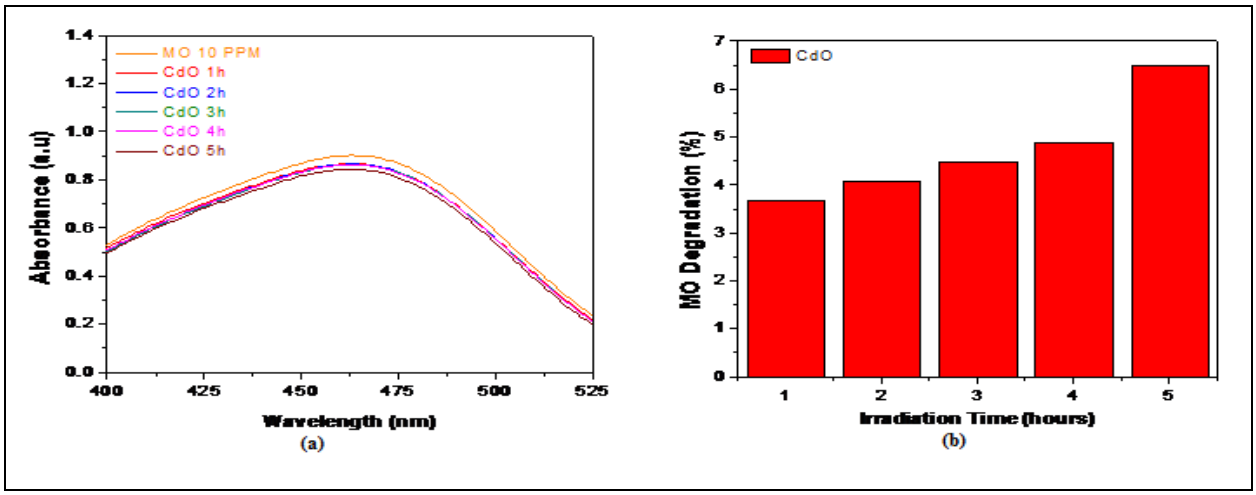

Fig. 5: (a) Absorbance of methyl orange by pure CdO thin films and (b) the corresponding bar chart

This may be because of the enhanced coverage of the semiconductor surface by the metal which diminishes the adsorption sites on the surface. Researchers have demonstrated that an enhanced photo-catalytic activity of doped-metal oxide is probably due to the acting of metal oxides to trap photo-induced electrons, retarding the electron–hole recombination process, and thereby promoting the photo degradation activity. Similarly, in this work, an enhanced photo catalytic activity of 3 wt. % Al-doped CdO system may be due to the Al atoms acting to trap photo-induced electrons, delaying the process of electron–hole recombination, and hence might have promoted the photo degradation activity. The degradation percentage is calculated for MB and MO individually and is tabulated in Table 2 and Table 3.

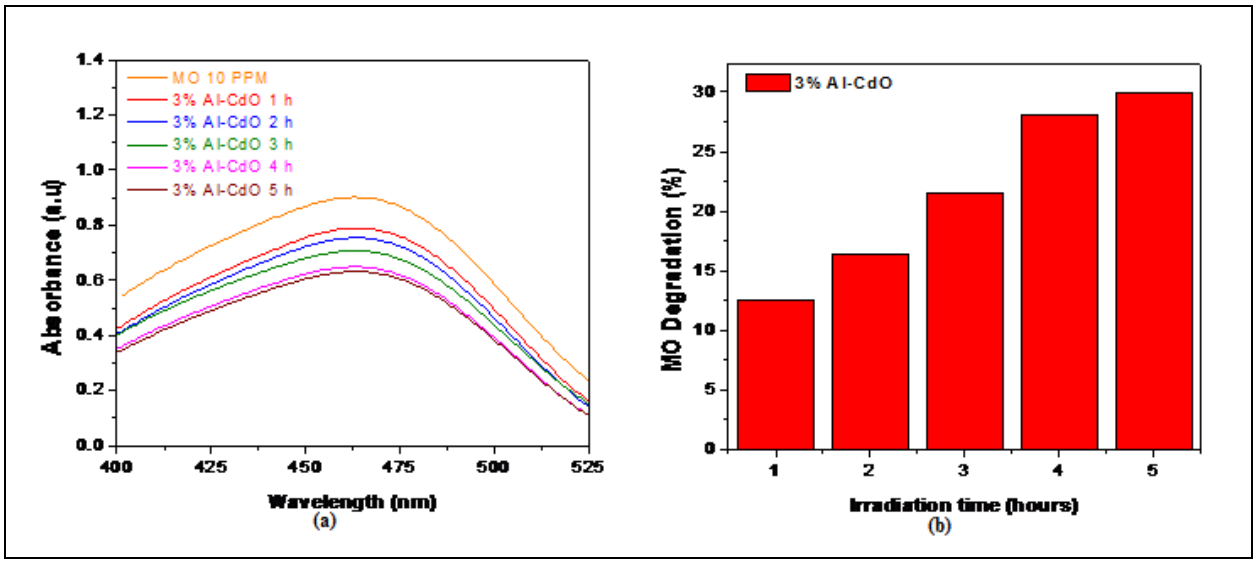

Fig. 6: (a) Absorbance of MO by 3 wt. % Al-doped CdO films and (b) the equivalent bar diagram

Table 2. Degradation % of MB

MB Degradation- CdO					
Time	**A_0**	**A_t**	**A_0-A_t**	**A_0-A_t/A_0**	**(A_0-A_t/A_0) * 100**
1h	2.7015	2.4039	0.2976	0.110161	11.0161
2h	2.7015	2.3708	0.3307	0.122413	12.2413
3h	2.7015	2.3377	0.3638	0.134666	13.4665
4h	2.7015	2.2716	0.4299	0.159134	15.9134
5h	2.7015	2.2165	0.485	0.17953	17.9530
MB Degradation 3% Al-CdO					
Time	**A_0**	**A_t**	**A_0-A_t**	**A_0-A_t/A_0**	**(A_0-A_t/A_0) * 100**
1h	2.886	2.7212	0.1648	0.057103	5.7103
2h	2.886	2.6382	0.2478	0.085863	8.5863
3h	2.886	2.5686	0.3174	0.109979	10.9976
4h	2.886	2.5376	0.3484	0.120721	12.0720
5h	2.886	2.3665	0.5195	0.180007	18.0007

Table 3. Degradation % of MO

MO Degradation CdO					
Time	**A_0**	**A_t**	**A_0-A_t**	**A_0-A_t/A_0**	**(A_0-A_t/A_0) * 100**
1h	0.9039	0.8708	0.0331	0.036619	3.6619
2h	0.9039	0.8671	0.0368	0.040712	4.0712
3h	0.9039	0.8634	0.0405	0.044806	4.4805
4h	0.9039	0.8598	0.0441	0.048789	4.8788
5h	0.9039	0.8451	0.0588	0.065051	6.5051
MO Degradation 3% Al-CdO					
Time	**A_0**	**A_t**	**A_0-A_t**	**A_0-A_t/A_0**	**(A_0-A_t/A_0) * 100**
1h	0.902	0.7896	0.1124	0.124612	12.4611
2h	0.902	0.7542	0.1478	0.163858	16.3858
3h	0.902	0.7084	0.1936	0.214634	21.4634
4h	0.902	0.6493	0.2527	0.280155	28.0155
5h	0.902	0.6315	0.2705	0.299889	29.9889

Once the aqueous semiconductor (CdO) solutions are irradiated in light energy greater than the bandgap energy of the semiconductors, conduction band electrons, and valence band holes are produced (Jiang *et al.* 2013; Lee *et al.* 2014). As the charge separation is sustained, the electrons and holes may drift to the semiconductor surface, where it takes part in the redox reaction with azo dyes (Zhao *et al.* 2013; Hamadanian *et al.* 2013; Harraz *et al.* 2014). The electrons generated by light react with the adsorbed dye molecules (O_2^-) on the semiconductor site and lessen it to superoxide radical anion (O_2^-) while the photogenerated holes oxidize the H_2O or OH^- ions adsorbed at the semiconductor surface to OH^- radicals (Priyanka *et al.* 2013; Shahmoradi *et al.* 2015). These radicals generated with other high-oxidant species work as strong oxidizing agents which could easily hit the adsorbed azo dye molecules or those located close to the surface of the semiconductor, thus resulting in the degradation of azoic dyes (Muhd Julkapli *et al.* 2014). Thus in the present work also, the degradation of azoic dyes might have been caused by the redox reaction on the semiconductor surface.

4. CONCLUSION

The obtained results demonstrated that the pure and Al-doped CdO thin films could degrade azoic dyes (methylene blue and methyl orange) with optimum conditions. It was found that 3 wt. % Al-doped CdO bleaches methylene blue much better with 19% degradation than the pure CdO thin films upon its exposure to the UV light. Among the two different azoic dyes, methyl orange reacts better, degrading to a aximum of 30%.

FUNDING

This research received no specific grant from any funding agency in the public, commercial, or not-for-profit sectors.

CONFLICTS OF INTEREST

The authors declare that there is no conflict of interest.

REFERENCES

Beydoun, Rose Amal and Gary Low, M., Role of nanoparticles in photocatalysis, *J. Nanopart. Res.*, 1(4), 439–456 (1999). http://dx.doi.org/10.1023/A:1010044830871

Borhade, A. V., Tope, D. R. and Uphade, B. K., An efficient photocatalytic degradation of methyl blue dye by using synthesised PbO nanoparticles, *E-J. Chem.*, 9(2), 705–715 (2012). http://dx.doi.org/10.1155/2012/362680

Cheng, M., Zhu, M., Du, Y. and Yang, P., Enhanced photocatalytic hydrogen evolution based on efficient electron transfer in triphenylamine-based dye functionalized Au@Pt bimetallic core/shell nanocomposite, *Int. J. Hydrog. Energy.*, 38(21), 8631–8638 (2013). http://dx.doi.org/10.1016/j.ijhydene.2013.05.040

Comparelli, R., Fanizza, E., Curri, M. L., Cozzoli, P. D., Mascolo, G. and Agostiano, A., UV-induced photocatalytic degradation of azo dyes by organic-capped ZnO nanocrystals immobilized onto substrates, *Appl. Catal. B Environ.*, 60(1–2), 01–11 (2005). http://dx.doi.org/10.1016/j.apcatb.2005.02.013

Hajjaji, A., Atyaoui, A., Trabelsi, K., Amlouk, M., Bousselmi, L., Bessais, B., El Khakani, M. A. and Gaidi, M., Cr-Doped TiO_2, Thin films prepared by means of a magnetron co-sputtering process: Photocatalytic application, *Am. J. Anal. Chem.*, 05(08), 473–482 (2014). http://dx.doi.org/ 10.4236/ajac.2014.58056

Hamadanian, M., Behpour, M., Razavian, A. S. and Jabbari, V., Structural, morphological and photocatalytic characterisations of Ag-coated anatase TiO_2 fabricated by the sol–gel dip-coating method, *J. Exp. Nanosci.*, 8(7–8), 901–912 (2013). http://dx.doi.org/10.1080/17458080.2011.620018

Harraz, F. A., Mohamed, R. M., Rashad, M. M. and Wang, Y. C., Sigmund, W., Magnetic nanocomposite based on titania–silica/cobalt ferrite for photocatalytic degradation of methylene blue dye, *Ceram. Int.*, 40(1), 375–384 (2014). http://dx.doi.org/10.1016/j.ceramint.2013.06.012

Hussein, F. H., Chemical properties of treated textile dyeing wastewater, *Asian J. Chem.*, 25(16), 9393–9400 (2013). http://dx.doi.org/10.14233/ajchem.2013.15909A

Jiang, T., Zhang, L., Ji, M., Wang, Q., Zhao, Q., Fu, X. and Yin, H., Carbon nanotubes/TiO_2 nanotubes composite photocatalysts for efficient degradation of methyl orange dye, *Particuology*, 11(6), 737–742 (2013). http://dx.doi.org/10.1016/j.partic.2012.07.008

Lajnef, W., Vinassa, J. M., Briat, O., Azzopardi, S. and Woirgard, E., Characterization methods and modelling of ultracapacitors for use as peak power sources, *J. Power Sources.*, 168(2), 553–560 (2007). http://dx.doi.org/10.1016/j.jpowsour.2007.02.049

Lee, H. U., Lee, G., Park, J. C., Lee, Y.-C., Lee, S. M., Son, B., Park, S. Y., Kim, C., Lee, S., Lee, S. C., Nam, B., Lee, J. W., Bae, D. R., Yoon, J.-S. and Lee, J., Efficient visible-light responsive TiO_2 nanoparticles incorporated magnetic carbon photocatalysts, *Chem. Eng. J.*, 240, 91–98 (2014). http://dx.doi.org/ 10.1016/j.cej.2013.11.054

Muhd Julkapli, N., Bagheri, S. and Bee Abd Hamid, S., Recent advances in heterogeneous photocatalytic decolorization of synthetic dyes, *Sci. World J.*, 01–25 (2014). http://dx.doi.org/10.1155/2014/692307

Nag, A., Sapra, S., Gupta, S. Sen, Prakash, A., Ghangrekar, A., Periasamy, N. and Sarma, D. D., Luminescence in Mn-doped CdS nanocrystals, *Bull. Mater. Sci.*, 31(3), 561–568 (2008). http://dx.doi.org/10.1007/s12034-008-0087-0

Priyanka and Srivastava, V. C., Photocatalytic oxidation of dye bearing wastewater by iron doped zinc oxide, *Ind. Eng. Chem. Res.*, 52(50), 17790–17799 (2013). http://dx.doi.org/10.1021/ie401973r

Rahman, M. M., Khan, B. S., Marwani, H. M., Asiri, A. M., Alamry, K. A., Rub, M. A., Khan, A., Khan, A. A. P. and Azum, N., Facile synthesis of doped ZnO – CdO nanoblocks as solid – phase adsorbent and efficient solar photocatalyst applications, *J. Ind. Eng. Chem.*, 20(4), 2278–2286 (2014). https://doi.org/10.1016/j.jiec.2013.09.059

Rajachandrasekar, T., Selvakumar, P.and Balakrishnan, K., Photocatalytic degradation of dichlorvos using graphite oxide based catalysts, *J. Environ. Nanotechnol.*, 5(2), 04–10 (2016). http://dx.doi.org/ 10.13074/jent.2016.06.162188

Saleh, T. A. and Gupta, V. K., Photo-catalyzed degradation of hazardous dye methyl orange by use of a composite catalyst consisting of multi-walled carbon nanotubes and titanium dioxide, *J. Colloid Interface Sci.*, 371(1), 101–106 (2012). http://dx.doi.org/10.1016/j.jcis.2011.12.038

Sarkar, S. and Chattopadhyay, K. K., Visible light photocatalysis and electron emission from porous hollow spherical $BiVO_4$ nanostructures synthesized by a novel route, *Physica E: Low Dimens. Syst. Nanostruct.*, 58, 52–58 (2014). https://doi.org/10.1016/j.physe.2013.11.014

Shahmoradi, B., Maleki, A. and Byrappa, K., Removal of disperse orange 25 using in situ surface-modified iron-doped TiO_2 nanoparticles, *Desalin. Water Treat.*, 53(13), 3615–3622 (2015). http://dx.doi.org/ 10.1080/19443994.2013.873994

Shiragami, T., Fukami, S. and Wada, Y., Semiconductor photocatalysis: effect of light intensity on nanoscale cadmium sulfide – catalyzed photolysis of organic substrates, *J. Phys. Chem*., 97(49), 12882–12887 (1993). https://dx.doi.org/10.1021/j100151a041

Soltani, T. and Entezari, M. H., Photolysis and photocatalysis of methylene blue by ferrite bismuth nanoparticles under sunlight irradiation, *J. Mol. Catal. A Chem.*, 377, 197–203 (2013). http://dx.doi.org/10.1016/j.molcata.2013.05.004

Sun, L., Shi, Y., Li, B., Li, X. and Wang, Y., Preparation and characterization of polypyrrole/TiO_2 nanocomposites reverse microemulsion polymerization and its photocatalytic activityfor degradation of methyl orange under natural light, *Polym. Compos.*, 34(7), 1076–1080 (2013). https://doi.org/10.1002/pc.22515

Tadjarodi, A., Imani, M., Kerdari, H., Bijanzad, K., Khaledi, D. and Rad, M., Preparation of CdO rhombus-like nanostructure and its photocatalytic degradation of azo dyes from aqueous solution, *Nanomater. Nanotechnol.*, 4, 16 (2014). http://dx.doi.org/10.5772/58464

Ullah, K., Meng, Z.-D., Ye, S., Zhu, L. and Oh, W.-C., Synthesis and characterization of novel PbS–graphene/TiO_2 composite with enhanced photocatalytic activity, *J. Ind. Eng. Chem.*, 20(3), 1035–1042 (2014). http://dx.doi.org/10.1016/j.jiec.2013.06.040

Zhao, W., Zhang, Y., Du, B., Wei, D., Wei, Q. and, Zhao, Y., Enhancement effect of silver nanoparticles on fermentative biohydrogen production using mixed bacteria, *Bioresour. Technol.*, 142, 240–245 (2013). http://dx.doi.org/10.1016/j.biortech.2013.05.042